Few-Body Systems 33, 219–232 (2003)
DOI 10.1007/s00601-003-0018-y

Few-Body Systems
Printed in Austria

Regarding Proton Form Factors

J. C. R. Bloch[1], A. Krassnigg[2], and C. D. Roberts[2]

[1] DFG Research Center "Mathematics for Key Technologies,"
c/o Weierstrass Institute for Applied Analysis and Stochastics, Mohrenstrasse 39,
D-10117 Berlin, Germany
[2] Physics Division, Argonne National Laboratory, Argonne, IL 60439-4843, USA

Received June 20, 2003; accepted September 12, 2003
Published online December 4, 2003;

Abstract. The proton's elastic electromagnetic form factors are calculated using an *ansatz* for the nucleon's Poincaré covariant Faddeev amplitude that only retains scalar diquark correlations. A spectator approximation is employed for the current. On the domain of q^2 accessible in modern precision experiments these form factors are a sensitive probe of nonperturbative strong interaction dynamics. The ratio of Pauli and Dirac form factors can provide realistic constraints on models of the nucleon and thereby assist in developing an understanding of nucleon structure.

1 Introduction

The pion's elastic electromagnetic form factor is accessible via a properly constructed six-point quark Schwinger function, a fact exploited with modest success in lattice-QCD simulations, e.g., refs. [1–3]. This Schwinger function is also the basis for continuum studies, among which those employing the Dyson-Schwinger equations (DSEs) [4–6] are efficacious [7]. The proton's form factors are accessible through an analogous eight-point quark Schwinger function, which is the starting point for lattice simulations, e.g., refs. [8, 9]. The fruitful extension of DSE methods to the calculation of this Schwinger function is a contemporary goal. As we will explain, a simple truncation that corresponds to a spectator approximation is currently in widespread use [10–12]. Manifest covariance is a strength of this approach for it has long been apparent that in order to obtain an internally consistent understanding of proton form factor data at spacelike momentum transfers $q^2 \gtrsim M^2$, where M is the proton's mass, a Poincaré covariant description of the scattering process is necessary [13, 14]. This has recently been reemphasized in the context of constituent-quark models [15–20].

The same interaction which describes the structure and properties of colour-singlet mesons also generates a quark-quark (diquark) correlation in the colour antitriplet ($\bar{3}$) channel [21, 22]. Such correlations have recently been observed in simulations of lattice-QCD [23]. While diquarks do not survive as asymptotic states [24–26]; viz., they do not appear in the strong interaction spectrum, the existence of strong quark-quark correlations provides a foundation for viewing the nucleon as a quark-diquark composite. This picture can be realized via a Poincaré covariant Faddeev equation [27], in which two quarks are always correlated as a $\bar{3}$-diquark, and binding in the nucleon is effected by the iterated exchange of roles between the dormant and diquark-participant quarks, and through the action of a pion ''cloud'' [28].

Upon solving the Faddeev equation one obtains the nucleon's mass, and also its Faddeev amplitude which is a valuable intuitive tool. It is noteworthy that even a rudimentary covariant Faddeev equation model, based on the presence of diquark correlations within the nucleon, yields a matrix-valued amplitude that, in the nucleon's rest frame, corresponds to a relativistic wave function with a material lower component; i.e., a wave function with ''p-wave'' and, indeed, ''d-wave'' correlations, too [29]. Nonzero quark orbital angular momentum in the nucleon is a straightforward outcome of a Poincaré covariant description.

While some issues remain unresolved [30, 31], contemporary data [32–34] suggest that a single dipole mass cannot simultaneously characterize the Q^2-dependence of both the proton's electric and magnetic form factors. This possibility was evident in the Faddeev-amplitude-based calculations of ref. [10], as emphasized in ref. [11]. Moreover, it can be inferred from ref. [35] that this experimental result is an essential consequence of a nonperturbative and Poincaré covariant representation of the proton as a bound state. This may be exemplified through the role played by pseudovector components of the pion's Bethe-Salpeter amplitude, which are connected with the presence of quark orbital angular momentum in the pion. These pseudovector amplitudes are necessarily nonzero [36] and responsible for the large-Q^2 behaviour of the electromagnetic pion form factor [37, 38].

Herein we calculate the proton's elastic electromagnetic form factors, using a product *ansatz* for the proton's Faddeev amplitude and a spectator approximation to describe elastic electromagnetic scattering from the nucleon. We describe the model in Sect. 2, and present and discuss the results in Sect. 3. Sect. 4 is an epilogue. The study furnishes a means by which we may explore and illustrate the points outlined above. It will become apparent that existing precision data on the form factor ratios $F_2^p(q^2)/F_1^p(q^2)$ and $G_E^p(q^2)/G_M^p(q^2)$ are a sensitive probe of nonperturbative aspects of the proton's structure.

2 Model Elements

2.1 Dressed Quarks

There are three primary elements of our model and to begin with its specification we note that quarks within bound states are described by a dressed

propagator[1]

$$S(p) = -i\gamma\cdot p\,\sigma_V(p^2) + \sigma_S(p^2) = \frac{1}{i\gamma\cdot p\,A(p^2) + B(p^2)} = \frac{Z(p^2)}{i\gamma\cdot p + M(p^2)}. \quad (1)$$

It is a longstanding, model-independent DSE prediction that the wave function renormalization $Z(p^2)$ and mass function $M(p^2)$ exhibit significant momentum dependence for $p^2 \lesssim 2\,\mathrm{GeV}^2$ whose origin is nonperturbative [4–6]. This behaviour was recently verified in numerical simulations of quenched QCD [39], and the connection between this and the full theory is analyzed in ref. [40].

The mass function is enhanced at infrared momenta, a feature that is an essential consequence of the dynamical chiral symmetry breaking (DCSB) mechanism. It is also the origin of the constituent-quark mass. With increasing spacelike p^2, on the other hand, the mass function evolves to reproduce the asymptotic behaviour familiar from perturbative analyses and that behaviour is manifest for $p^2 \gtrsim 10\,\mathrm{GeV}^2$ [41].

While numerical solutions for the dressed-quark propagator are readily obtained from a model of QCD's gap equation, the utility of an algebraic form for $S(p)$, when calculations require the evaluation of numerous multidimensional integrals, is self-evident. An efficacious parametrization, which exhibits the features described above and has been used extensively [4–6], is expressed via

$$\bar\sigma_S(x) = 2\bar m\,\mathcal{F}(2(x+\bar m^2)) + \mathcal{F}(b_1 x)\,\mathcal{F}(b_3 x)\,[b_0 + b_2\mathcal{F}(\epsilon x)], \quad (2)$$

$$\bar\sigma_V(x) = \frac{1}{x+\bar m^2}\left[1 - \mathcal{F}(2(x+\bar m^2))\right], \quad (3)$$

with $x = p^2/\lambda^2$, $\bar m = m/\lambda$,

$$\mathcal{F}(x) = \frac{1-e^{-x}}{x}, \quad (4)$$

$\bar\sigma_S(x) = \lambda\,\sigma_S(p^2)$ and $\bar\sigma_V(x) = \lambda^2\,\sigma_V(p^2)$. The mass-scale, $\lambda = 0.566\,\mathrm{GeV}$, and parameter values[2]

$$\begin{array}{ccccc} \bar m & b_0 & b_1 & b_2 & b_3 \\ \hline 0.00897 & 0.131 & 2.90 & 0.603 & 0.185 \end{array}, \quad (5)$$

were fixed in a least-squares fit to light-meson observables [42]. The dimensionless $u = d$ current-quark mass in Eq. (5) corresponds to

$$m = 5.1\,\mathrm{MeV}. \quad (6)$$

The parametrization yields a Euclidean constituent-quark mass

$$M^E_{u,d} = 0.33\,\mathrm{GeV}, \quad (7)$$

[1] We employ a Euclidean metric wherewith the scalar product of two four-vectors is $a\cdot b = \sum_{i=1}^4 a_i b_i$, and Hermitean Dirac-$\gamma$ matrices that obey $\{\gamma_\mu,\gamma_\nu\} = 2\delta_{\mu\nu}$

[2] $\epsilon = 10^{-4}$ in Eq. (2) acts only to decouple the large- and intermediate-p^2 domains

defined as the solution of $p^2 = M^2(p^2)$ [41], whose magnitude is typical of that employed in constituent-quark models [43]. This is an expression of DCSB, as is the vacuum quark condensate

$$-\langle\bar{q}q\rangle_0^{1\,\mathrm{GeV}^2} = \lambda^3\,\frac{3}{4\pi^2}\,\frac{b_0}{b_1\,b_3}\,\ln\frac{1\,\mathrm{GeV}^2}{\Lambda_{\mathrm{QCD}}^2} = (0.221\,\mathrm{GeV})^3, \tag{8}$$

$\Lambda_{\mathrm{QCD}} = 0.2\,\mathrm{GeV}$. The condensate is calculated directly from its gauge invariant definition [36] after making allowance for the fact that Eqs. (2) and (3) yield a chiral-limit quark mass function with anomalous dimension $\gamma_m = 1$. This omission of the additional $\ln(p^2/\Lambda_{\mathrm{QCD}}^2)$-suppression that is characteristic of QCD is merely a practical simplification.

2.2 *Product Ansatz for the Faddeev Amplitude*

We represent the proton as a composite of a dressed-quark and nonpointlike, Lorentz-scalar quark-quark correlation (diquark), and exhibit this via a product *ansatz* for the Faddeev amplitude

$$\Psi_3^{0^+}(p_i,\alpha_i,\tau_i) = \left[\Gamma^{0^+}\left(\tfrac{1}{2}p_{[12]};K\right)\right]_{\alpha_1\alpha_2}^{\tau_1\tau_2}\,\Delta^{0^+}(K)\,[\mathcal{S}(\ell;P)u(P)]_{\alpha_3}^{\tau_3}, \tag{9}$$

wherein (p_i,α_i,τ_i) are the momentum, spin, and isospin labels of the quarks constituting the nucleon; the spinor satisfies

$$\bar{u}(P)\,(i\gamma\cdot P + M) = 0 = (i\gamma\cdot P + M)\,u(P), \tag{10}$$

with $P = p_1 + p_2 + p_3$ the nucleon's total momentum, and it is also a spinor in isospin space with $\varphi_+ = \mathrm{col}(1,0)$ for the proton and $\varphi_- = \mathrm{col}(0,1)$ for the neutron; and $K = p_1 + p_2 =: p_{\{12\}}$, $p_{[12]} = p_1 - p_2$, $\ell := (-p_{\{12\}} + 2p_3)/3$.

In Eq. (9), $\Delta^{0^+}(K)$ is a pseudoparticle propagator for the scalar diquark formed from quarks 1 and 2, and Γ^{0^+} is a Bethe-Salpeter-like amplitude describing their relative momentum correlation. These functions can be obtained from an analysis of the quark-quark scattering matrix, as explained in ref. [28]. However, we have already chosen to simplify our calculations by parametrizing $S(p)$, and hence we follow refs. [10, 11] and also employ that expedient herein, using

$$\Delta^{0^+}(K) = \frac{1}{m_{0^+}^2}\,\mathcal{F}(K^2/\omega_{0^+}^2), \tag{11}$$

$$\Gamma^{0^+}(k;K) = \frac{1}{\mathcal{N}^{0^+}}\,H\,C i\gamma_5\,i\tau_2\,\mathcal{F}(k^2/\omega_{0^+}^2), \tag{12}$$

with $\mathcal{F}$ defined in Eq. (4), $C = \gamma_2\gamma_4$ the charge conjugation matrix, τ_2 the 2×2 Pauli isospin matrix, and $(H^{c_3})_{c_1c_2} = \epsilon_{c_1c_2c_3}$, $c_{1,2,3} = 1,2,3$, describing the completely antisymmetric colour structure of a $\bar{3}$ diquark.[3] The parameters are a width, ω_{0^+}, and a pseudoparticle mass, m_{0^+}, which have ready physical interpretations: The length $l_{0^+} = 1/\omega_{0^+}$ is a measure of the mean separation between the quarks in

[3] In Eq. (12), $\mathcal{N}^{0^+}$ is a calculated normalization constant which ensures that a (ud)-diquark has electric charge fraction $(1/3)$ for $K^2 = -m_{0^+}^2$. $\mathcal{N}_\Psi$, to appear in Eq. (15), is analogous: It is the calculated normalization constant that ensures the proton has unit charge

the scalar diquark; and the distance $\lambda_{0^+} = 1/m_{0^+}$ represents the range over which a diquark correlation in this channel can persist inside the nucleon.

With the elements described hitherto it is possible to derive a Poincaré covariant Faddeev equation whose solution yields $\mathcal{S}$, a 4×4 Dirac matrix that describes the relative quark-diquark momentum correlation. The complete nucleon amplitude then follows:

$$\Psi = \Psi_1 + \Psi_2 + \Psi_3, \tag{13}$$

where the subscript identifies the dormant quark and, e.g., $\Psi_{1,2}$ are obtained from Ψ_3 by a uniform, cyclic permutation of all the quark labels. The general form of $\mathcal{S}$ is discussed at length in ref. [29] with the conclusion that the positive energy solution can be written

$$\mathcal{S}(\ell;P) = f_1(\ell;P)\, I_{\rm D} + \frac{1}{M}\left(i\gamma\cdot\ell - \ell\cdot\hat{P}\, I_{\rm D}\right) f_2(\ell;P), \tag{14}$$

where $(I_{\rm D})_{rs} = \delta_{rs}$, $\hat{P}^2 = -1$. In the nucleon's rest frame, $f_{1,2}$, respectively, describe the upper, lower component of the spinor amplitude $\mathcal{S}(\ell;P)\, u(P)$.

Again, calculations are simplified if one employs an algebraic parametrization of $\mathcal{S}$, and the form [44]

$$\mathcal{S}(\ell;P) = \frac{1}{\mathcal{N}_\Psi}\, \mathcal{F}(\ell^2/\omega^2_{q\{qq\}}) \left[I_{\rm D} - \frac{\mathrm{R}}{M}\left(i\gamma\cdot\ell - \ell\cdot\hat{P}\, I_{\rm D}\right)\right] \tag{15}$$

is efficacious. In writing this one exploits results of the Faddeev equation calculations reported in refs. [28, 29], which establish the fidelity of the approximations $f_2(\ell;P) \approx \mathrm{R}\, f_1(\ell;P)$ and $f_1(\ell;P) \approx f_1(\ell^2;P^2)$. The *ansatz* involves two parameters: a width $\omega_{q\{qq\}}$ and ratio R. The former can be associated with a length-scale $l_{q\{qq\}} = 1/\omega_{q\{qq\}}$, which measures the quark-diquark separation. The latter gauges the importance of the lower component of the positive energy nucleon's spinor amplitude. Its magnitude increases with increasing R. (The strength of the lower component of the nucleon's Faddeev *wave function* is determined by R but does not vanish for $\mathrm{R} = 0$.) In realistic Faddeev equation studies of the nucleon $l_{q\{qq\}} > l_{0^+}/2 \sim 0.2\,$fm and $\mathrm{R} \sim 0.5$ [28].

2.3 Dressed-Quark-Photon Coupling

A calculation of the electromagnetic interaction of a composite particle cannot proceed without an understanding of the coupling between the photon and the bound state's constituents. If those constituents are dressed then the coupling is not pointlike. Indeed, it is readily apparent that with quarks dressed as described in Sect. 2.1, only a dressed-quark-photon vertex, Γ_μ, can satisfy the vector Ward-Takahashi identity:

$$q_\mu\, i\Gamma_\mu(\ell_1,\ell_2) = S^{-1}(\ell_1) - S^{-1}(\ell_2), \tag{16}$$

where $q = \ell_1 - \ell_2$ is the photon momentum flowing into the vertex. This is illustrated with particular emphasis in refs. [38, 45–50], which consider effects associated with the Abelian anomaly. The Ward-Takahashi identity is only one of many constraints that apply to Γ_μ in a renormalizable quantum field theory and these have been explored extensively in refs. [51, 52].

The dressed-quark-photon vertex, a three-point Schwinger function, can be obtained by solving an inhomogeneous Bethe-Salpeter equation. This was the procedure adopted in the DSE calculation [7] that successfully predicted the electromagnetic pion form factor [53]. For our purposes, however, it is enough to follow ref. [42] and employ the algebraic parametrization [54]

$$i\Gamma_\mu(\ell_1,\ell_2) = i\Sigma_A(\ell_1^2,\ell_2^2)\,\gamma_\mu + (\ell_1+\ell_2)_\mu\Big[\tfrac{1}{2}i\gamma\cdot(\ell_1+\ell_2)\,\Delta_A(\ell_1^2,\ell_2^2) + \Delta_B(\ell_1^2,\ell_2^2)\Big]; \tag{17}$$

with

$$\Sigma_F(\ell_1^2,\ell_2^2) = \tfrac{1}{2}[F(\ell_1^2)+F(\ell_2^2)], \qquad \Delta_F(\ell_1^2,\ell_2^2) = \frac{F(\ell_1^2)-F(\ell_2^2)}{\ell_1^2-\ell_2^2}, \tag{18}$$

where $F = A, B$; i.e., the scalar functions in Eq. (1). It is critical that Γ_μ in Eq. (17) satisfies Eq. (16) and very useful that it is completely determined by the dressed-quark propagator. Improvements to this *ansatz* modify results by $\lesssim 10\%$, as illustrated, e.g., in refs. [55, 56].

Eq. (17) entails that dressed-quarks do not respond as point particles to low momentum transfer probes. This observation qualitatively supports an assumption employed in some relativistic constituent quark models [13, 15, 57]. An unambiguous quantitative connection is difficult because the definition of constituent-quark degrees of freedom depends on a model's formulation. It may nevertheless be worth noting that quark dressing disappears with increasing spacelike q^2 in QCD. Hence, in the ultraviolet, the dressed-quark's Dirac form factor must approach one (with only $\ln q^2$ corrections) and its Pauli form factor must vanish; viz., the interaction becomes pointlike in this limit. With the parameter values in Eq. (5), this evolution of the Dirac and Pauli form factors may be characterized by monopole ranges $r_1 \sim 0.25\,\mathrm{fm}$ and $r_2 \sim 0.35\,\mathrm{fm}$, respectively.

2.4 Commentary

We have completely specified a covariant model of the nucleon as a bound state of a dressed-quark and nonpointlike scalar quark-quark correlation. This algebraic *ansatz* has four parameters: m_{0^+} and ω_{0^+} introduced in Eqs. (11) and (12) to characterize the diquark; and $\omega_{q\{qq\}}$ and R in Eq. (15), which express prominent features of the nucleon's spinor. The dressed-quark propagator and dressed-quark-photon vertex are fixed.

In contemplating such a model one may ask whether it *can* supply an accurate description of the nucleon's electromagnetic form factors. *A priori*, the answer is unknown but it is supplied by straightforward calculations.

A more important question, however, is whether the model *should* be accurate. In this case the answer is *no*. Reference [28] emphasizes that no picture of the nucleon is veracious if it neglects axial-vector diquark correlations and the nucleon's pion "cloud." Thus our simple model must be incomplete. Fortunately, estimates exist of the contributions made by these terms to the nucleon's electromagnetic properties [12, 58–60], and in the following they are used to inform the model's application.

3 Calculated Form Factors

The nucleon's electromagnetic current is

$$J_\mu(P', P) = ie\,\bar{u}(P')\,\Lambda_\mu(q, P)\,u(P), \tag{19}$$

$$= ie\,\bar{u}(P')\left(\gamma_\mu F_1(q^2) + \frac{1}{2M}\,\sigma_{\mu\nu}\,q_\nu\,F_2(q^2)\right)u(P), \tag{20}$$

where $q = P' - P$ and Λ_μ is the nucleon-photon vertex described in the Appendix. In Eq. (20), F_1 and F_2 are, respectively, the Dirac and Pauli electromagnetic form factors. They are the primary calculated quantities, from which one obtains the nucleon's electric and magnetic form factors

$$G_E(q^2) = F_1(q^2) - \frac{q^2}{4M^2}F_2(q^2), \qquad G_M(q^2) = F_1(q^2) + F_2(q^2). \tag{21}$$

To proceed with the illustration we select two values of R, namely, $\mathrm{R} = 0.25$, 0.50. This choice is motivated by Faddeev equation studies, in which the smaller value is obtained by calculations that retain scalar and axial-vector diquark correlations but neglect the pion cloud, while the latter is obtained if the estimated effect of that cloud is incorporated [28]. Then, in each case, we fix the remaining three parameters by requiring a least-squares fit to

$$G_E^p(q^2) = 1/(1 + q^2/m_d^2)^2, \tag{22}$$

with $m_d = 1.1\,\mathrm{GeV}$. This value of the dipole mass corresponds to a proton charge radius $r_p = 0.62\,\mathrm{fm}$; i.e., $\sim 30\%$ smaller than the experimental value, and therefore leaves room deliberately for additional contributions to the nucleon's electromagnetic structure from axial-vector diquark correlations and a meson "cloud." While the leading nonanalytic contribution to r_p can alone repair the discrepancy [58, 60], that does not alter the quiddity of our scheme because the scale of the effect is clear and redistributing strength between complementary contributions can be achieved merely by fine-tuning the model's parameters.

In Table 1 we list the parameter values produced by this fitting procedure along with the calculated values of proton and neutron static properties. The proton's

Table 1. Fitted model parameters and calculated nucleon static properties. The values indicate: $\lambda_{0^+} = 1/m_{0^+} \sim \frac{1}{3}$ fm, $l_{0^+} = 1/\omega_{0^+} \sim \frac{1}{7}$ fm, $l_{q\{qq\}} = 1/\omega_{q\{qq\}} \sim \frac{2}{3}$ fm. For comparison, the third row lists values of the parameters determined in ref. [28] by solving the Faddeev equation with the inclusion of axial-vector diquark correlations and allowing for a pion cloud contribution; and the last row provides experimental values of the static quantities

	Parameters				Calculated Static Properties			
	R	m_{0^+} (GeV)	ω_{0^+}	$\omega_{q\{qq\}}$	$(r_p^2)^2$ (fm^2)	$(r_n^2)^2$	μ_p (μ_N)	μ_n
	0.25	0.75	1.50	0.33	$(0.65)^2$	$-(0.38)^2$	2.58	−1.39
	0.50	0.77	1.42	0.29	$(0.61)^2$	$-(0.37)^2$	2.52	−1.37
Ref. [28]	0.54	0.74	0.45	0.44				
Obs.					$(0.87)^2$	$-(0.34)^2$	2.79	−1.91

charge radius is precisely that for which we aimed. However, the values of the remaining static properties point to the deficiencies of a model that retains only a scalar diquark correlation. They confirm that in this case one is unable to obtain a quantitatively accurate picture of the nucleon. This is reassuring because, in contributing to nucleon observables, axial-vector diquark correlations primarily interfere constructively with the pion cloud; e.g., they both provide additional binding and hence act to reduce the nucleon's mass [28], and they both act to increase $|\mu_{p,n}|$, $|r^2_{p,n}|$ [12, 58–60]. Hence a model that ignores these contributions but succeeds in fitting experimental data is likely to possess spurious degrees of freedom.[4] In the table's third row we list values of this model's parameters that were determined differently; viz., in a study [28] that allows for pion cloud contributions to the nucleon's mass and solves a Faddeev equation whose kernel admits axial-vector diquark correlations. In comparing these values with those in the first two rows it is apparent that only the value of ω_{0^+} is materially different. One may therefore conclude that attempting to fit physical observables with a scalar diquark alone leads to a correlation that is too pointlike; i.e., $l_{0^+} = 1/\omega_{0^+}$ is too small. The improvements necessary to make the model more realistic are therefore plain. In their absence it is nevertheless possible to illustrate important points.

A first observation relates to what may be called the nucleon's ''quark core.'' In an internally consistent model it is always possible to identify the relative strength of various contributions to a physical observable. For example, ref. [28] employs a rainbow-dressed quark and ladder-bound meson basis, within which the quark core contributes approximately 85% of the nucleon's mass. In the present case an estimate of the core's spatial extent is afforded by $l_{q\{qq\}} = 1/\omega_{q\{qq\}} \approx \frac{2}{3}$ fm, which is commensurate with our calculated core contribution to the proton's charge radius, Table 1. It will also be evident that this scale is consistent with estimates of the magnitude of meson-loop contributions to the proton's charge radius determined from lattice-QCD simulations [58, 60].

We depict the proton's Dirac form factor in the left panel of Fig. 1, wherein it is clear that the shift in parameter values has little observable impact. That is also true for the Pauli form factor, which is plotted in the right panel. These two functions together give the proton's electric form factor, via Eq. (21), and that is shown in Fig. 2.

We plot the calculated ratio: $F_2/\kappa F_1$, $\kappa = \mu_p - 1$, in Fig. 3, along with modern experimental data [32, 34]. In addition, we draw the calculated result for this ratio obtained using the parameter values of the scalar diquark *ansatz* employed in ref. [10]. These values: $\mathrm{R} = 0.0$, and (in GeV) $m_{0^+} = 0.63$, $\omega_{0^+} = 1.4$, $\omega_{q\{qq\}} = 0.2$, were fixed via a least-squares fit to Eq. (22) but with $m_d = 0.84\,\mathrm{GeV}$, which gives $r_p = 0.87\,\mathrm{fm}$. The figure illustrates that the ratio decreases smoothly with increasing R, bracketing the data, and thereby suggests that even the rudimentary *ansatz* is capable of accurately describing the data. Indeed, the $\mathrm{R} = 0.25$ parameter set might

[4] The implementation of current conservation in the one-body current described in the Appendix is too simple to allow a fair description of G^n_E. In this case it misses important cancellations and hence we report anomalously large values for $|r^2_n|$. A realistic description requires a more complex current which includes fully-fledged seagull terms [12]. The simple current is adequate for the remaining form factors because such destructive interference is either absent or markedly less important [10]

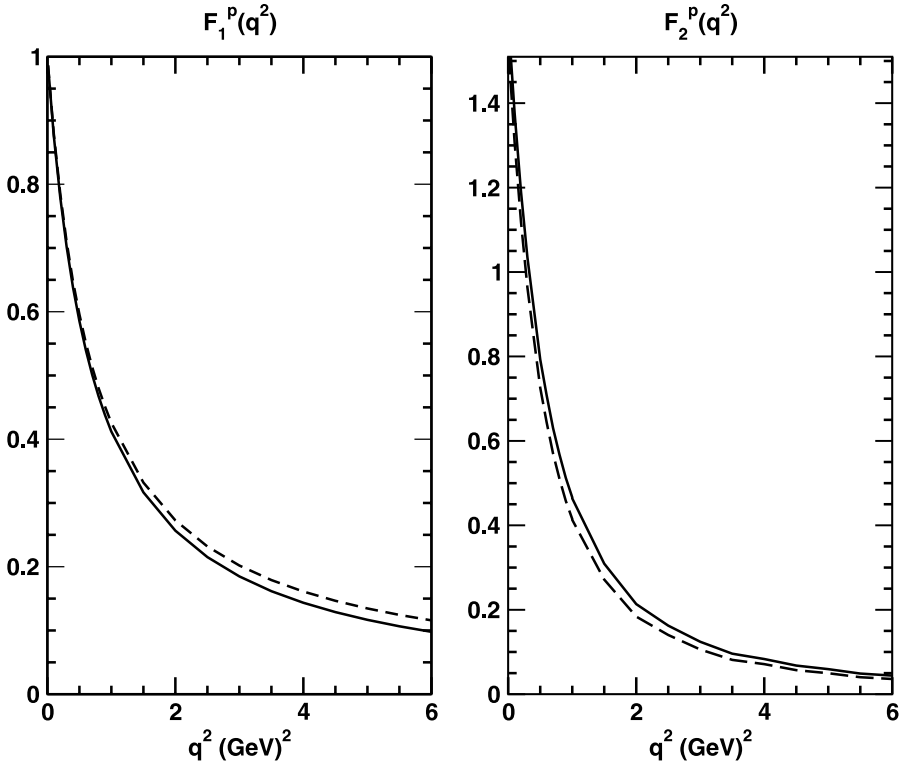

Fig. 1. Left panel: Calculated proton Dirac form factor. Right panel: Calculated proton Pauli form factor. Solid line, R = 0.25; dashed, R = 0.50. The associated model parameters are listed in Table 1

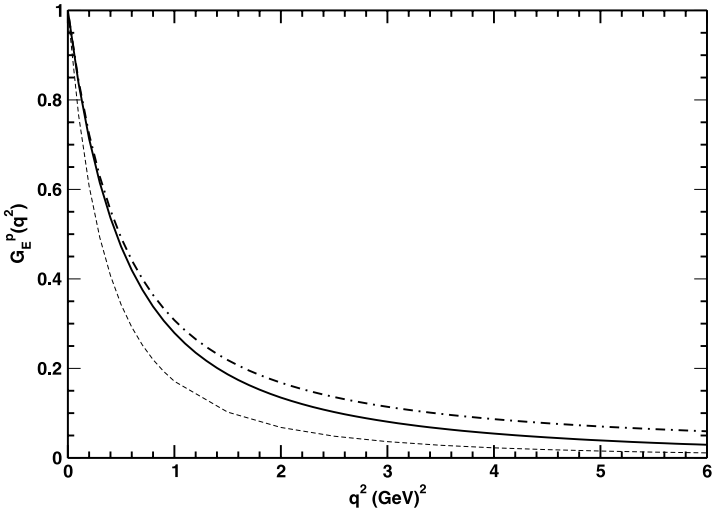

Fig. 2. Calculated proton electric form factor: solid line, R = 0.25; dot-dashed, R = 0.50 – the associated model parameters are listed in Table 1. For comparison, the lighter dashed line is $G_E^p(q^2) = 1/(1 + q^2/m^2_{\mathrm{emp-p}})^2$, $m_{\mathrm{emp-p}} = 0.84\,\mathrm{GeV}$; viz., a dipole fit to available proton data

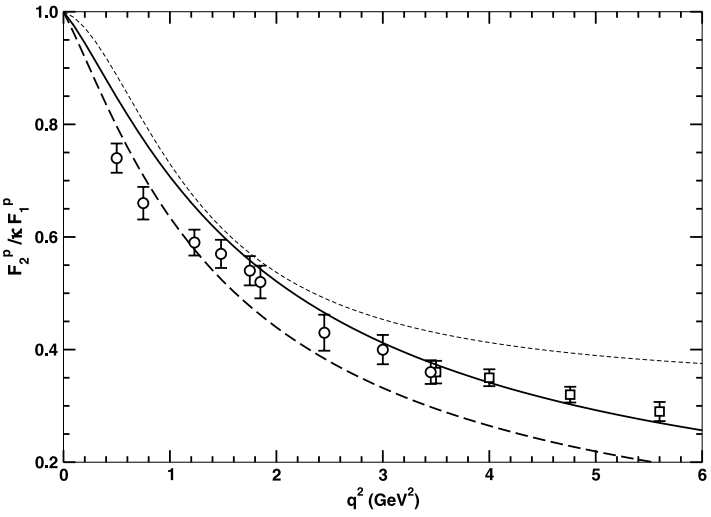

Fig. 3. Calculated ratio $F_2^p/(\kappa F_1^p)$, $\kappa = \mu_p - 1$: solid line, R = 0.25; dashed, R = 0.50 – the associated model parameters are listed in Table 1. The short-dashed line was obtained with the model parameters in ref. [10]: R = 0.0, and (in GeV) $m_{0^+} = 0.63$, $\omega_{0^+} = 1.4$, $\omega_{q\{qq\}} = 0.2$. Data: boxes, ref. [32]; circles, ref. [34]

even be considered a good representation. However, this is not the conclusion we draw. Rather, the result demonstrates that the available data on this ratio is sensitive to model-dependent details.

The ratio $\mu_p G_E^p/G_M^p$ is depicted in Fig. 4 and therein the last statement is amplified. The proton's electric form factor is a difference, Eq. (21), and that accentuates its sensitivity. On the domain for which data is available, this ratio

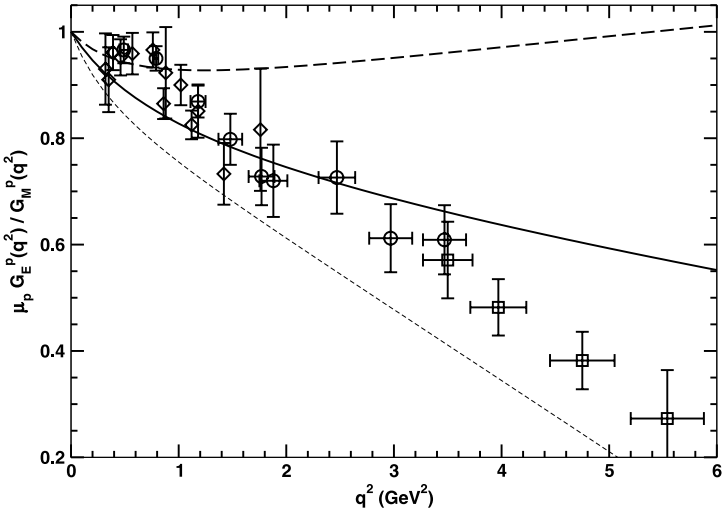

Fig. 4. Calculated ratio $\mu_p G_E^p(q^2)/G_M^p(q^2)$: solid line, R = 0.25; dashed, R = 0.50 – the associated model parameters are listed in Table 1. The lighter short-dashed line was obtained with the model parameters in ref. [10]: R = 0.0, and (in GeV) $m_{0^+} = 0.63$, $\omega_{0^+} = 1.4$, $\omega_{q\{qq\}} = 0.2$. Data: boxes, ref. [32]; diamonds, ref. [33]; circles, ref. [34]

is particularly responsive to model details, a result also conspicuous in ref. [12]. It is plain that three parameter sets, which are reasonable and differ modestly when compared through the ratio $F_2/\kappa F_1$, appear vastly different in the comparison presented in Fig. 4. Moreover, because of continuity, it is clear that one could tune the model parameters to fit the data on this ratio. However, what might be considered success in that endeavour could easily be achieved through results for G_E^p and G_M^p individually which both disagree with the data.

4 Summary and Discussion

We calculated the proton's elastic electromagnetic form factors using a rudimentary *ansatz* for the nucleon's Poincaré covariant Faddeev amplitude that represents the proton as a composite of a confined quark and confined nonpointlike scalar diquark. All such models give a Faddeev wave function that corresponds to a nucleon spinor with a sizeable lower component in the rest frame.

This study indicates that on the domain of q^2 accessible in modern precision experiments these form factors are a sensitive probe of nonperturbative dynamics. The calculated pointwise forms express a dependence on the length-scales that characterize nonperturbative phenomena, such as bound state extent, dressing of quark and gluon propagators, and meson cloud effects. This is precisely analogous to the current status of the pion's electromagnetic form factor, for which the behaviour predicted in a straightforward application of perturbative QCD is not unambiguously evident until $q^2 \gtrsim 15\,\mathrm{GeV}^2$ [38].

The ratio $\mu_p G_E^p/G_M^p$ is particularly sensitive to infrared dynamics because, as q^2 increases, $G_E^p(q^2)$ is a difference of small quantities. However, this ratio should not be considered in isolation because it is possible to reproduce the experimental data using a model that simultaneously provides a poor description of the individual form factors. That is also true of the ratio $F_2^p/\kappa F_1^p$ but this combination is less responsive to model particulars because the Dirac and Pauli form factors are positive and fall uniformly to zero, with a momentum dependence at asymptotically large momenta given by perturbative QCD [62, 63]. In the absence of a veracious theoretical understanding of the nucleon, we view the latter ratio as a more sensible constraint on contemporary studies.

It is apparent that much can be learnt about long-range dynamics in QCD from existing and forthcoming accurate data on nucleon form factors. In constraining systematic QCD-based calculations, one can hope, for example, to see an evolution from the domain on which meson cloud effects are important to that whereupon observables are dominated by the confined quark core. This could be elucidated by improving the present study; viz., basing it on a solution of the Poincaré covariant Faddeev equation with axial-vector diquark correlations, instead of using an *ansatz* for the Faddeev amplitude, and explicitly including meson cloud contributions. The form factors would then be tied directly to assumptions about the nature of quark-gluon dynamics in the nucleon.

Acknowledgement. We are grateful to M. B. Hecht for helpful correspondence and for providing us with his computer code; and to F. Coester and T.-S. H. Lee for constructive discussions. This work was supported by: the Department of Energy, Nuclear Physics Division, under contract no. W-31-109-ENG-38;

the Austrian Research Foundation FWF under Erwin-Schrödinger-Stipendium no. J2233-N08; and benefited from the resources of the National Energy Research Scientific Computing Center.

Appendix A: Nucleon-Photon Vertex

We use an *ansatz* for Ψ_3 in the nucleon's Faddeev amplitude, Eq. (13), from which a properly antisymmetrized one-body vertex can be constructed via the method outlined in ref. [4],

$$\Lambda_\mu(q,P) = \Lambda^1_\mu(q,P) + 2\sum_{i=2}^{5} \Lambda^i_\mu(q,P), \tag{A.1}$$

wherein

$$\Lambda^1_\mu(q,P) = 3\int \frac{d^4\ell}{(2\pi)^4}\, \mathcal{S}\left(\ell - \frac{2}{3}q; P\right) \Delta^{0^+}(K)\, \mathcal{S}(\ell;P)\, \Lambda^S_\mu(p_3+q,p_3), \tag{A.2}$$

with $K = \ell + \frac{2}{3}P$, $p_3 = \frac{1}{3}P - \ell$, $\Lambda^S_\mu(\ell_1,\ell_2) = S(\ell_1)\,\Gamma^Q_\mu(\ell_1,\ell_2)\,S(\ell_2)$; and

$$\Lambda^2_\mu(q,P) = 6\int \frac{d^4k}{(2\pi)^4}\frac{d^4\ell}{(2\pi)^4}\, \Omega(p_1+q,p_2,p_3)\, \Omega(p_1,p_2,p_3)\, \mathrm{tr}_{DF}\left[\Lambda^S_\mu(p_1+q,p_1)S(p_2)\right] S(p_3), \tag{A.3}$$

where $p_1 = \frac{1}{2}K + k$, $p_2 = \frac{1}{2}K - k$, $6 = \varepsilon_{c_1c_2c_3}\varepsilon_{c_1c_2c_3}$ is the colour contraction, and

$$\Omega(p_1,p_2,p_3) = \Delta^{0^+}(p_{\{12\}})\,\Gamma_{0^+}\left(\tfrac{1}{2}p_{[12]}; p_{\{12\}}\right) \mathcal{S}\left(\tfrac{1}{3}[p_{\{12\}} - 2p_3]; P\right). \tag{A.4}$$

Λ^2_μ describes the photon probing the structure of the scalar diquark correlation, and contributes equally to both the proton and neutron. The remaining terms are

$$\begin{aligned}\Lambda^3_\mu(q,P) = 6\int \frac{d^4k}{(2\pi)^4}\frac{d^4\ell}{(2\pi)^4}\, &\Omega(p_1,p_2,p_3) \\ &\times\ \Omega(p_1+q,p_3,p_2)\, S(p_2)\, (i\tau_2)^{\mathrm{t}} \Lambda^S_\mu(p_1,p_1+q)\, (i\tau_2)\, S(p_3),\end{aligned} \tag{A.5}$$

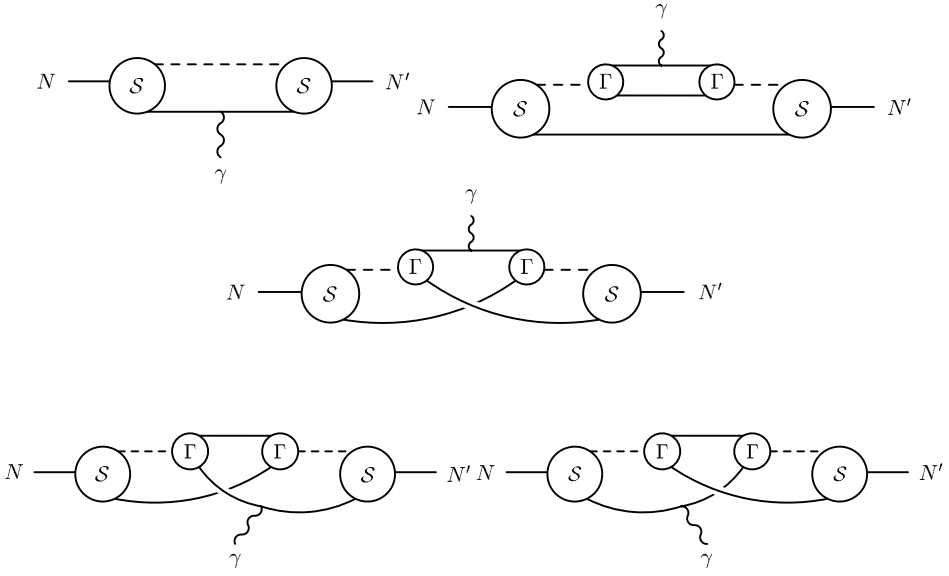

Fig. A.1. One-body current obtained from the product *ansatz* of Eq. (9). Solid line, dressed-quark propagator $S(p)$; dashed line, diquark propagator $\Delta^{0^+}(K)$. The amputated nucleon vertex is $\Psi^{0^+}_3$ in every case

where "t" denotes matrix transpose, and

$$\Lambda^4_\mu(q,P) = 6\int \frac{d^4k}{(2\pi)^4}\frac{d^4\ell}{(2\pi)^4}\,\Omega(p_1,p_3,p_2+q)\,\Omega(p_1,p_2,p_3)\,\Lambda^S_\mu(p_2+q,p_2)\,S(p_1)\,S(p_3), \qquad \text{(A.6)}$$

$$\Lambda^5_\mu(q,P) = 6\int \frac{d^4k}{(2\pi)^4}\frac{d^4\ell}{(2\pi)^4}\,\Omega(p_1,p_3+q,p_2)\,\Omega(p_1,p_2,p_3)\,S(p_2)\,S(p_1)\,\Lambda^S_\mu(p_3+q,p_3). \qquad \text{(A.7)}$$

We illustrate these five terms in Fig. A.1. They are in one-to-one correspondence with those considered in ref. [61], with the bottom two diagrams, representing $\Lambda^{4,5}_\mu$, being progenitors of the "seagull" terms exploited therein to ensure current conservation.

Our results are obtained by evaluating these integrals using Monte-Carlo methods and the input specified in Eqs. (2), (3), (11), (12), (15), and (17).

References

1. Martinelli, G., Sachrajda, C. T.: Nucl. Phys. **B306**, 865 (1988)
2. Draper, T., Woloshyn, R. M., Wilcox, W., Liu, K. F.: Nucl. Phys. **B318**, 319 (1989)
3. van der Heide, J., Lutterot, M., Koch, J. H., Laermann, E.: Phys. Lett. **B566**, 131 (2003)
4. Roberts, C. D., Schmidt, S. M.: Prog. Part. Nucl. Phys. **45**, S1 (2000)
5. Alkofer, R., Smekal, L. v.: Phys. Rept. **353**, 281 (2001)
6. Maris, P., Roberts, C. D.: Int. J. Mod. Phys. **E12**, 297 (2003)
7. Maris, P., Tandy, P. C.: Phys. Rev. **C61**, 045202 (2000)
8. Martinelli, G., Sachrajda, C. T.: Nucl. Phys. **B316**, 355 (1989)
9. Göckeler, M., et al.: Nucleon Electromagnetic Form Factors on the Lattice and in Chiral Effective Field Theory; hep-lat/0303019
10. Bloch, J. C. R., Roberts, C. D., Schmidt, S. M., Bender, A., Frank, M. R.: Phys. Rev. **C60**, 062201 (1999)
11. Bloch, J. C. R., Roberts, C. D., Schmidt, S. M.: Phys. Rev. **C61**, 065207 (2000)
12. Oettel, M., Alkofer, R., Smekal, L. v.: Eur. Phys. J. **A8**, 553 (2000)
13. Chung, P. L., Coester, F.: Phys. Rev. **D44**, 229 (1991)
14. Coester, F.: Prog. Part. Nucl. Phys. **29**, 1 (1992)
15. Pace, E., Salme, G., Molochkov, A.: Nucl. Phys. **A699**, 156 (2002)
16. Simula, S.: Phys. Rev. **C66**, 035201 (2002)
17. Boffi, S., et al.: Eur. Phys. J. **A14**, 17 (2002)
18. Desplanques, B., Theussl, L.: Eur. Phys. J. **A13**, 461 (2002)
19. Miller, G. A.: Phys. Rev. **C66**, 032201 (2002)
20. Cardarelli, F., Simula, S.: Phys. Rev. **C62**, 065201 (2000)
21. Cahill, R. T., Roberts, C. D., Praschifka, J.: Phys. Rev. **D36**, 2804 (1987)
22. Maris, P.: Few-Body Systems **32**, 41 (2002)
23. Hess, M., Karsch, F., Laermann, E., Wetzorke, I.: Phys. Rev. **D58**, 111502 (1998)
24. Bender, A., Roberts, C. D., Smekal, L. v.: Phys. Lett. **B380**, 7 (1996)
25. Hellstern, G., Alkofer, R., Reinhardt, H.: Nucl. Phys. **A625**, 697 (1997)
26. Bender, A., Detmold, W., Roberts, C. D., Thomas, A. W.: Phys. Rev. **C65**, 065203 (2002)
27. Cahill, R. T., Roberts, C. D., Praschifka, J.: Austral. J. Phys. **42**, 129 (1989)
28. Hecht, M. B., Oettel, M., Roberts, C. D., Schmidt, S. M., Tandy, P. C., Thomas, A. W.: Phys. Rev. **C65**, 055204 (2002)
29. Oettel, M., Hellstern, G., Alkofer, R., Reinhardt, H.: Phys. Rev. **C58**, 2459 (1998)
30. Brash, E. J., Kozlov, A., Li, S., Huber, G. M.: Phys. Rev. **C65**, 051001 (2002)
31. Arrington, J.: Phys. Rev. **C68**, 034325 (2003)
32. Jones, M. K., et al. [JLab Hall A Collaboration]: Phys. Rev. Lett. **84**, 1398 (2000)

33. Gayou, O., et al.: Phys. Rev. **C64**, 038202 (2001)
34. Gayou, O., et al. [JLab Hall A Collaboration]: Phys. Rev. Lett. **88**, 092301 (2002)
35. Gousset, T., Pire, B., Ralston, J. P.: Phys. Rev. **D53**, 1202 (1996)
36. Maris, P., Roberts, C. D., Tandy, P. C.: Phys. Lett. **B420**, 267 (1998)
37. Farrar, G. R., Jackson, D. R.: Phys. Rev. Lett. **43**, 246 (1979)
38. Maris, P., Roberts, C. D.: Phys. Rev. **C58**, 3659 (1998)
39. Bowman, P. O., Heller, U. M., Williams, A. G.: Phys. Rev. **D66**, 014505 (2002)
40. Bhagwat, M. S., Pichowsky, M. A., Roberts, C. D., Tandy, P. C.: Phys. Rev. **C68**, 015203 (2003)
41. Maris, P., Roberts, C. D.: Phys. Rev. **C56**, 3369 (1997)
42. Burden, C. J., Roberts, C. D., Thomson, M. J.: Phys. Lett. **B371**, 163 (1996)
43. Capstick, S., Roberts, W.: Prog. Part. Nucl. Phys. **45**, S241 (2000)
44. Hecht, M. B., Roberts, C. D., Schmidt, S. M.: Phys. Rev. **C64**, 025204 (2001)
45. Bando, M., Harada, M., Kugo, T.: Prog. Theor. Phys. **91**, 927 (1994)
46. Roberts, C. D.: Nucl. Phys. **A605**, 475 (1996)
47. Alkofer, R., Roberts, C. D.: Phys. Lett. **B369**, 101 (1996)
48. Kekez, D., Klabučar, D.: Phys. Lett. **B457**, 359 (1999)
49. Roberts, C. D.: Fizika **B8**, 285 (1999)
50. Tandy, P. C.: Fizika **B8**, 295 (1999)
51. Bashir, A., Kızılersü, A., Pennington, M. R.: Phys. Rev. **D57**, 1242 (1998)
52. Bashir, A., Kızılersü, A., Pennington, M. R.: Analytic Form of the One-Loop Vertex and of the Two-Loop Fermion Propagator in 3-Dimensional Massless QED; hep-ph/9907418
53. Volmer, J., et al. [JLab F_π Collaboration]: Phys. Rev. Lett. **86**, 1713 (2001)
54. Ball, J. S., Chiu, T.-W.: Phys. Rev. **D22**, 2542 (1980)
55. Pichowsky, M. A., Walawalkar, S., Capstick, S.: Phys. Rev. **D60**, 054030 (1999)
56. Alkofer, R., Bender, A., Roberts, C. D.: Int. J. Mod. Phys. **A10**, 3319 (1995)
57. Cardarelli, F., Pace, E., Salme, G., Simula, S.: Phys. Lett. **B357**, 267 (1995)
58. Leinweber, D. B., Cohen, T. D.: Phys. Rev. **D47**, 2147 (1993)
59. Hackett-Jones, E. J., Leinweber, D. B., Thomas, A. W.: Phys. Lett. **B489**, 143 (2000)
60. Hackett-Jones, E. J., Leinweber, D. B., Thomas, A. W.: Phys. Lett. **B494**, 89 (2000)
61. Oettel, M., Pichowsky, M. A., Smekal, L. v.: Eur. Phys. J. **A8**, 251 (2000)
62. Lepage, G. P., Brodsky, S. J.: Phys. Rev. Lett. **43**, 545 (1979) [Erratum: Phys. Rev. Lett. **43**, 1625 (1979)]
63. Lepage, G. P., Brodsky, S. J.: Phys. Rev. **D22**, 2157 (1980)